Multi-objective flower pollination algorithm: a new technique for EEG signal denoising

Zaid Abdi Alkareem Alyasseri[1,2] · Ahamad Tajudin Khader[3] · Mohammed Azmi Al-Betar[4,5] ·
Xin-She Yang[6] · Mazin Abed Mohammed[7] · Karrar Hameed Abdulkareem[8] · Seifedine Kadry[9] ·
Imran Razzak[10]

Abstract

The electroencephalogram (EEG) signal denoising problem has been considered a challenging task because of several artifact noises, such as eye blinking, eye movement, muscle activity, and power line interference, which can corrupt the original EEG signal during the recording time. Therefore, to remove these noises, the EEG signals must be processed to obtain efficient EEG features. Accordingly, several techniques have been proposed to reduce EEG noises, such as EEG signal denoising using wavelet transform (WT). The success of WT depends on the best configuration of its control parameters, which are often experimentally set. In this study, a multi-objective flower pollination algorithm (MOFPA) with WT (MOFPA-WT) is proposed to solve the EEG signal denoising problem. The novelty of this study is to find optimal EEG signal denoising parameters using MOFPA based on two measurement criteria for the denoised signals, namely minimum mean squared error (MSE) and maximum signal-to-noise ratio (SNR). The MOFPA-WT is tested using a standard EEG signal processing dataset, namely the EEG motor movement/imagery dataset. The performance of MOFPA-WT is evaluated using five criteria, namely SNR, SNR improvement, MSE, root mean squared error (RMSE), and percentage root mean square difference (PRD). Experiments are conducted using FPA with MSE, SNR, and MSE and SNR to show the effect of the multi-objective aspects on the performance of the proposed MOFPA-WT. Results show that FPA with MSE and SNR exhibits more subjective results than FPA with MSE and FPA with SNR. The convergence rate and Pareto front are also studied for the proposed MOFPA-WT.

Keywords Electroencephalogram · Signal denoising · Wavelet transform · Multi-objective · Flower pollination algorithm

1 Introduction

The electroencephalogram (EEG) signal denoising is considered a challenge due to various noises in the artifact such as eye blinking, eye motion, muscle activity, and interference with power line that can alter the original EEG signal during the recording time. Therefore, the EEG signals must be processed to achieve efficient EEG usability in order to eliminate these noises. Several techniques to reduce EEG noises such as EEG signal denoising by wavelet transform (WT) were recommended. Wavelet transform's success depends on how best its control parameters are configured and often set experimentally. Various algorithms for optimizing configurations are used

to find optimal WT parameters such as β-hill climbing [1]. Flower pollination algorithm (FPA) is classified as a natural-inspiring algorithm based on the flowering plants' pollination behavior. The FPA is established by Yang in 2012 [2]. The FPA has adhered successfully for a number of optimization problems and is outperformed some selected algorithms in a previous study [3, 4]. Yang et al. [5] mooted an initial attempt to extend FPA by a random weighted sum method to deal with multi-objective engineering optimization problems (MOFPA). The MOFPA has been assessed to achieve optimum results using a few engineering optimization problems. Subsequently the same authors proposed a novel MOFPA technique [6], with several multi-objective tests functions and two bi-objective design benchmarks. Compared with other algorithms the outcomes of the proposed algorithm were highly efficient. The MOFPA has been used to tackle real world issues such

Extended author information available on the last page of the article

as the radial distribution system [7], dynamic economic dispatch in consideration of emissions [8], transmission losses and power plant emissions, cost reduction, increased voltage stabilization [9], power loss reduction [10], and power influx problem [11].

This paper mainly aims to propose an efficient EEG signal denoising technique using a multi-objective flower pollination algorithm with wavelet transform (MOFPA-WT). The (MOFPA-WT) method is used to obtain the best parameters combination for EEG signal denoising by means of two objective functions, *min(MSE)* and *max(SNR)*. The proposed method is used to combine several objectives into a composite one-objective function in accordance with a weighted sum approach. The original EEG signal is from the standard EEG dataset, *Motor Movement/Imagery dataset*[1] [12]. This set of data consists of 109 volunteers, and record EEG signals from 64 EEG channels based on mental tasks. The results of denoised EEG signal are assessed in terms of five measurement factors for the evaluation of the MOFPA-WT, namely SNR, SNR improvement, MSE, RMSE and PRD. It should be noted that in comparison to those methods based on FPA-MSE and FPA-SNR, the proposed method MOFPA-WT achieves efficient EEG signal denoising based on all criteria.

This paper has been arranged in the following sections. Section 2 provides an EEG background and its applications. Section 3 explains a wavelet transform and EEG wavelet-based denoising. Section 4 discusses the background of the flower pollination algorithm (FPA). Section 5 provides a description of the MOFPA-WT for tuning WT parameters. In Sect. 6 we describe the results and the discussion. Lastly, Sect. 7 outlines the conclusion and future work.

2 Electroencephalogram (EEG)

Electroencephalogram (EEG) is an electric brain activity graph recorded from the scalp. This recording shows variability in voltage resulting from ionic fluxes within the brain's neurons [13–15]. EEG signals can, therefore, generate a lot information needed on brain activity. Brain EEG signals are captured by *invasive* or *noninvasive* methods [16, 17]. The major difference among these techniques is the use of electrode arrays in the brain, such as *ECoG BCI* for arm motion control, as the invasive method [18]. In the meantime, there are a range of techniques for recording brain activities, including EEG for electrical activity of scalp, MEGs for magnetic field fluctuations in the brain and

fMRI and fNIR for changes in oxygenation level in blood resulting from neural activity [18].

H. Berger first suggested the noninvasive EEG signals could be used to collect brain activities [19]. Researchers have developed the technique of Berger for a variety of applications over several decades. In clinical applications, for example, EEG signals were used for prevention, diagnosis-detection, rehabilitation, and patient restoration. The method is also used in non-medical applications like education and self-regulation, neuromarketing and advertisements, smart environment and neuroergonomics, games and entertainment, as well as education and learning [20–22]. EEG signals have recently successfully been employed in safety and authentication applications as a new biometric technique [13, 20, 23, 24].

More than one artifact noises, such as eye blinking, eye movement, muscle activity and electronic device intervention, could typically corrupt the original EEG signal during the recording time [25]. Consequently, to reduce such noise, the EEG signal need to be manipulated. Various EEG noise elimination techniques like filtering and adaptive thresholding were suggested in the literature. WT was well adapted to denoise non-stationary signals, including ECG and EEG, in the last several years [1, 26–34].

The wavelet denoising has five parameters with different ranges of each parameter (Table 1). The efficiency of EEG signal denoising depends on the selection of the optimal combination of WT parameters. Usually, the parameters are selected based on experience or empirical evidence. In past studies, the configuration of the WT parameter is formulated to optimize MSE as its objective function [1, 32].

El-Dahshan tried to achieve an optimal configuration of wavelet denoising parameters by a genetic algorithm (GA) in [26], for ECG signals. The outcomes of its WT-based GA were better than any of those generated experimentally. Nguyen et al. in [35] suggested a genetically adaptive thresholding method for ECG signal denoising. They have used a MIT-BIH set of data [36] to test their method, which corrupts the original ECG signal with white Gaussian noise (WGN) and various SNR input noise levels. MSE and SNR were used to evaluate the performance of this procedure. WGN has effectively been eliminated from the ECG signal through their method. In order to acquire the optimum wavelet parameters, Alyasseri et al. [29] suggested that an ECG signal denoisation system based on β-hill climbing(β-hc) optimization with wavelet denoising be implemented [37]. Subsequently, the same authors used their hybrid techniques for EEG signals, and successfully obtained the optimal wavelet denoising parameters for non-stationary signals, like ECG and EEG [1, 31, 32].

---

[1]

Table 1 WT Parameters of signal denoising ranges

Wavelet denoising parameters	Method (range)
Mother wavelet function (MWF) Φ	**Coiflet** (coif1..coif5), **Daubechies** (db1..db45), **Symlet** (sym1..sym45), and **Biorthogonal** (bior1.1.. bior1.5 & bior2.2 .. bior2.8& bior3.1..bior3.9).
Thresholding function β	Soft(s) or hard(h)
Decomposition level L	Five
Thresholding selection rule λ	Minimax, Heursure, Sqtwolog, and Rigsure
Rescaling approach ρ	Mln, sln, and one

The wavelet denoising has distinct advantages to denoise the non-stationary signal such as the ECG and the EEG [38]. However, there is still a problem with the current efforts when it is used for signal denoising. The major drawback for the current version is that sometimes the noise is decreased and the power of the original signal is exhausted. This is normally the case in the denoising process, as previous work has solely sought to obtain a minimum (MSE) denoising EEG signal. This is why the authors propose to develop a multi-objective function that balance the power of the denoted EEG signal by using the maximum SNR, which will reduce the mean squared error.

3 EEG denoising using wavelet transform (WT)

The wavelet transform (WT) is a powerful and common tool for the representation of time frequency domain signals. WT has been applied successfully for signal compression, function selection and other applications [29, 39]. The WT can usually be categorized in two types: the discrete wavelet transform (DWT) and the continuous wavelet transform (CWT) [40]. Over the last few years, the WT has been widely applied in non-stationary signals like ECG and EEG, since several EEG artifact effects are proven harmful to the original EEG signal. These noises originated from eye blinking, eye movements, muscles activity, power line and EMG [34, 41–43]. This paper employs the DWT to denoise EEG signal. One of the methods for DWT is applied in [44] and so-called Donoho's approach. Thus, the DWT is defined as follows [45]:

$$C(a,b) = \sum_{n \in Z} x(n) g_{j,k}(n) \tag{1}$$

where $C(a,b)$ denotes the wavelet dynamic coefficients, $a = 2^{-j}$, $b = k2^{-j}$, $j \in Z$, $k \in Z$, Z is the set of integers; a is the size of the time scale, b is the translation, $x(n)$ is the input EEG signal, and $g_{j,k}(n) = 2^{j/2} g(2^j n - k)$ is the DWT.

DWT's task is to degrade the input signal by means of various coefficients, to correct both the high and low input signal frequencies. Figure 1 shows the denoising process of the wavelet with three decomposition levels (L=5).

In general, the wavelet denoising process has three phases which are summarized as follows:

- EEG signal *decomposition*, the original EEG signal is decomposed into five levels. The EEG signal is divided up into two parts on each level namely Approximation coefficients (cA), and Detail coefficients (cD). The cD will process using high-pass filter and cA will continue decompose for next level.
- ***Thresholding*** where a threshold value is defined for each level according to the noise level coefficients.
- ***Reconstruction***, the EEG denoised signal is reconstructed using inverse discrete wavelet transform ***iDWT***.

The wavelet denoising contains five parameters with different types of parameters (Table 1). Noise reduction efficiency depends on the choice of wavelet parameters. As
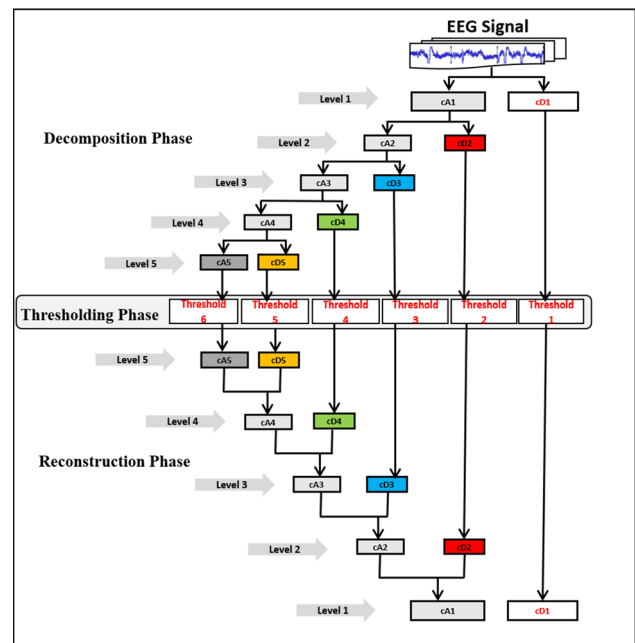

Fig. 1 EEG denoising process

shown in Fig. 1, the process of wavelet denoising has three phases. The first stage involves the **decomposition** of the EEG signal by DWT. In this stage, the right mother wavelet function (Φ) is chosen to be utilized for the EEG signal decomposition task. The second WT parameter, i.e., decomposition level (L), is normally based upon the EEG signal and experience in this phase. The selection of the WT valuable parameters (one of the key objectives of this paper) has recently been carried out using FPA and GA optimizing techniques.

In the second phase, **thresholding** is applied. The wavelet has two standard thresholds (β), i.e., a threshold that is **hard (h)** and **soft (s)** [44, 46]. The distinction between hard and soft thresholding is shown in Fig. 2. All threshold type (**soft** (s) or **hard** (**h**)), the rules of selection (λ), and the methods of rescalation (ρ) are to be chosen. These threshold mechanisms must be implemented as the choice will affect the overall performance of denoising. The thresholding value is usually based on the amplitude of noise (σ) [26]. The various parameters for thresholding selection rule and rescaling methods are shown in Tables 2 and 3. Finally, Equation (2) is used for the thresholding rules.

$$s(n) = x(n) + \sigma e(n) \tag{2}$$

where $x(n)$ is the original EEG signal, e is the noise, σ is the amplitude of the noise, and n is sample number. The wavelet parameters (β, λ, and ρ) must be separately applied for each wavelet coefficient (cA and cD) level. In the last phase, the denoised EEG signal is reconstructed by **iDWT**.

4 Flower pollination algorithm

According to [47], meta-heuristic algorithms can be categorized as evolutionary algorithms [48, 49], swarm intelligence [50–54], and trajectory algorithm [29, 37, 55, 56].

FPA is a successful swarm-based intelligence based on the pollination behavior of flowering plants. FPA was
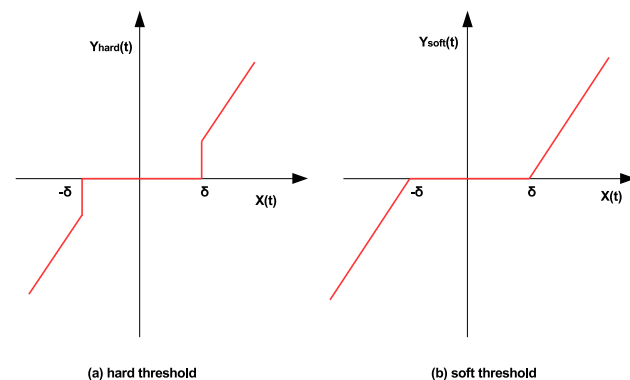

(a) hard threshold   (b) soft threshold

Fig. 2 Soft and hard thresholding methods

introduced by Yang in 2012 [2] and has been successfully applied for many optimization problems [3]. The operators (rules) of FPA are summarized as follows:

- **Operator (1)**: Global pollination encompasses biotic and cross-pollination where pollinators carry pollens based on Levy flights.
- **Operator (2)**: Local pollination necessitates abiotic and self-pollination.
- **Operator (3)**: The probability of reproduction can be seen as the flower constancy which is commensurate to the similarity of any two flowers.
- **Operator (4)**: The switch probability $p \in [0, 1]$ can be controlled between global and local pollination. Due to certain external factors, e.g., wind, local pollination will play a major part in the overall pollination activity.

These rules are described in further detail in the following subsection.

4.1 Global search of FPA (biotic)

As previously indicated, pollens of the flowers are transferred to long distances through this type of pollination, by bees, bats, birds, etc. This ensures that the most fit element is pollinated and reproduced. We can thus mathematically represent the first and third rules of the FPA as follows:

$$x_i^{itr+1} = x_i^{itr} + L_{dis}(g^* - x_i^{itr}) \tag{3}$$

where x_i^{itr+1} the pollen i or solution vector x_i at iteration itr, and g^* is the current best solution found among all solutions at the current iteration. The parameter L_{dis} is the strength of the pollination, which essentially is a step size. Since insects may move over a long distance with various distance steps, we can use a Levy flight to mimic this characteristic efficiently [2, 3, 57]. That is, we can use a Levy flight to imitate this feature effectively

$$L_{dis} \sim \frac{\lambda \Gamma(\lambda) sin(\pi\lambda/2)}{\pi} \frac{1}{s^{1+\lambda}}, (s >> s\_0 > 0) \tag{4}$$

$\Gamma(\lambda)$ denotes the standard gamma function, and this distribution is valid for large steps $s > 0$. In all our simulations below, we have used $\lambda = 1.5$.

4.2 Local search of FPA (abiotic)

There is no pollinator in this type of pollination, where it centered on the wind and diffusion to shift the pollen. The local pollination (**Operator 2**) and flower constancy (**Operator 3**) can be represented as follows:

$$x_i^{itr+1} = x_i^{itr} + \epsilon(x_j^{itr} - x_k^{itr}) \tag{5}$$

where x_j^{itr} and x_k^{itr} are pollens from the different flowers of the same plant type. This essentially mimic the flower constancy in a limited neighborhood. Mathematically, if x_j^{itr} and x_k^{itr} come from the same species or selected from the same population, this become a local random walk if we draw ϵ from a uniform distribution in [0,1].

4.3 Switch probability in FPA

This is the key feature of the FPA algorithm, because the performance of the FPA will effect according to the p value, where its value will determine which path will follow either global or local pollination. According to [2], the value of p can be used $p = 0.8$ to achieve the best results for most applications.

5 Proposed MOFPA with wavelet transform (WT) for denoising electroencephalogram (EEG) signals

This section provides a discussion of the proposed MOFPA with WT (MOFPA-WT) to solve EEG signal denoising problem (see Algorithm 1). WT parameter setting is crucial to yield efficient denoising results. Therefore, wavelet denoising parameters setting is formulated as an optimization problem. In our previous attempt, the optimal parameter setting for wavelet denoising were found by FPA, in which mean squared error (MSE) was used as an objective function [1, 58]. Aside from MSE, signal-to-noise (SNR) can also evaluate the quality of any solution. SNR is another important criterion for evaluation that should be considered.

Yang et al. in [6] claimed that any problem must be initially solved using single-objective function before adopting multi-objective functions. Therefore, EEG signal denoising problem was adopted using a single-objective function in [1, 58]. In the present study, the proposed method MOFPA-WT runs through four phases, where the result of each phase is an input to the succeeding one. Figure 3 shows the flowchart of these phases and thoroughly described as follows:

Algorithm 1 Tuning WT parameters using MOFPA for EEG signal denoising

1: Initialize noisy EEG signal ($Noisy_{eeg}$), and calculate the evaluation measures (SNR, MSE, root mean squared error (RMSE), and percentage root mean square difference (PRD) for input EEG signal).
2: Initialize MOFPA operators, and initialize solutions $Sol_i (i = 1, 2, .., D)$ D = 5 wavelet parameters,
   and the initial solution $Sol_i(\Phi, L, \beta, \lambda, \rho)$
3: Sol'_{opt} = MOFPA (X, Sol_i)
4: $EEG_{denoised}$ = WT $(Sol'_{opt}, Noisy_{eeg})$
5: EEGOutSignals = Evaluate($EEG_{denoised}, SNR_{out}, SNR_{imp}$, MSE, RMSE, PRD).

Phase I: *Initialization of EEG signals and WT parameters*. This phase involves three steps. First, the input EEG signal $x(n)$ is read from the source. The WT denoising approach was developed based on an original EEG signal being corrupted by three noises, namely white Gaussian noise (WGN), power line noise (PLN), and electromyogram (EMG) estimation [26, 59, 60] the corrupted formulas of which are shown in Eqs. (6), (8), and (10), respectively. These types of noises simulate the noises that will corrupt the original EEG signal during the recording time, such as eye blinking, eye movement, and electro signal distortion. Figure 4 shows the original EEG signal and noisy EEG signals.

$$\text{Noise}_{\text{PLN}} = x(n) + N_{\text{PLN}}(n) \tag{6}$$

where $N_{\text{PLN}}(n)$ is

$$N_{\text{PLN}}(n) = A * sin(2 * \pi * f * t) \tag{7}$$

$$\text{Noise}_{\text{EMG}} = x(n) + N_{\text{EMG}}(n) \tag{8}$$

where $N_{\text{EMG}}(n)$ is defined as follows:

$$N_{\text{EMG}}(t) = A * rand(n), rand \in [0, 1] \tag{9}$$

$$\text{Noise}_{\text{WGN}} = x(n) + N_{\text{WGN}}(n) \tag{10}$$

where $N_{\text{WGN}}(n)$ is

$$N_{\text{WGN}}(t) = x(n) + \sigma e(n) \tag{11}$$

where $A = 0.15$ uV, $f = 50$ Hz, e is the noise, and σ is the amplitude of the noise in this work $\sigma=15$ μV. N_{PLN}, N_{EMG}, and N_{WGN} signals are added to the original EEG signal $x(n)$ to simulate the actual noises.

Second, WT denoising parameters are initialized (i.e., Φ, L, β, λ, and ρ) which are shown in Table 1, as well as the parameters of MOFPA are also initialized as shown in Table 5. Finally, the input EEG signals are evaluated in terms of SNR by Eq. (14), PRD by Eq. (18), MSE by Eq. (13), and RMSE by Eq. (17) to record the results of EEG signals before and after the denoising process.

Table 2 Selection options of wavelet thresholding

Thresholding option	Description
Option 1: Sqtwolog	The threshold is chosen equal to $\sqrt{(2logM)}$ where M is number of coefficient in series
Option 2: Minimaxi	The threshold is chosen equal to **Max(MSE)**
Option 3: Rigrsure	The threshold is chosen based on the Stein Unbiased Risk Assessment (SURE) principle.
Option 4: Heursure	The threshold is chosen based on the mixture (**Sqtwolog** and **Rigrsure**)

Table 3 Rescaling approaches of the wavelet thresholding

threshold techniques ρ	rescaling
sln	Single level
mln	Multiple levels
one	No scaling

Phase II: **Tuning WT parameters using MOFPA.** This phase is the core work of this paper. The performance of WT depends on its initial parameters. Therefore, MOFPA is used to find the optimal parameters configuration. Initially, the solution of WT parameters configuration is represented as a vector $Sol = (s_1, s_2, \ldots s_D)$, where D is the total number of parameters used for WT, which is normally equal to 5. s_1 represents the value of the mother wavelet function (MWF) parameter Φ, s_2 denotes the value of the decomposition level parameter L, s_3 refers to the thresholding method β, s_4 represents the value of the thresholding selection rule parameter λ, and s_5 represents the re-scaling approach ρ; the possible ranges for these parameters are selected from Table 1.

Figure 5 shows an example of selection of the optimal solution of WT parameters for denoising EEG signals using MOFPA. The final result of this phase is an optimized solution $Sol'_{opt} = (s'_1, s'_2, \ldots s'_D)$, which will be passed onto the next phase.

The process of tuning WT parameters by using MOFPA is summarized as follows.

1. Initialize a set of solutions from the possible ranges of WT parameters using MOFPA. Moreover, initialize the switch probability in FPA P.
2. Calculate the two objective functions (i.e., $min(MSE)$, $Max(SNR)$) for all solutions and determine the current best solution ($g*$) to be used for the global pollination

later. For the local pollination, the solution will be selected randomly from the population.

3. Generate the rnd value and compare it with the switch probability in FPA P to manipulate the current solution (X_i) with global or local pollination to create the new solution (X'_i).
4. Evaluate the new solution (X'_i); if an improvement is observed, replace it with the current solution (X_i) and proceed to the next solution (X_{i+1}). Repeat Steps 3 and 4 for all solution. The proposed MOFPA-WT evaluates the solution using the multi-objective function, which is formulated in Eq. (12). This method is applied using two objective functions, namely **min(MSE)** and **max(SNR)** to achieve the best combination of WT parameters for EEG signal denoising.

$$F_{MOFPAWT} = (W_1 * \mathbf{min}(MSE)) + (W_2 * \mathbf{max}(SNR)) \tag{12}$$

$$MSE = \frac{1}{N} \sum_{n=1}^{N} [x(n) - \widehat{x}(n)]^2 \tag{13}$$

$$SNR_{out} = 10 \log_{10} \left\{ \frac{\sum_{n=1}^{N} [x(n)]^2}{\sum_{n=1}^{N} [x(n) - \widehat{x}(n)]^2} \right\}, \tag{14}$$

where $x(n)$ denotes the original EEG signal, and $\widehat{x}(n)$ is the denoised EEG signal obtained by tuning the wavelet parameters using MOFPA.

5. Update the current best solution ($g*$).
6. Repeat Steps 3–5 based on Max_{itr}
7. The Pareto optimal set contains the set of solution with the best value for two objective functions (i.e., $min(MSE)$, $max(SNR)$) or at least one objective function. Finally, the Pareto front solution will be selected from the Pareto optimal set (best solution in the Pareto optimal set).

Phase III: **EEG denoising using WT based on Sol'_{opt}.** As mentioned in Sect. 3, the denoising process of WT involves three main steps, as shown in Fig. 1 and described as follows.
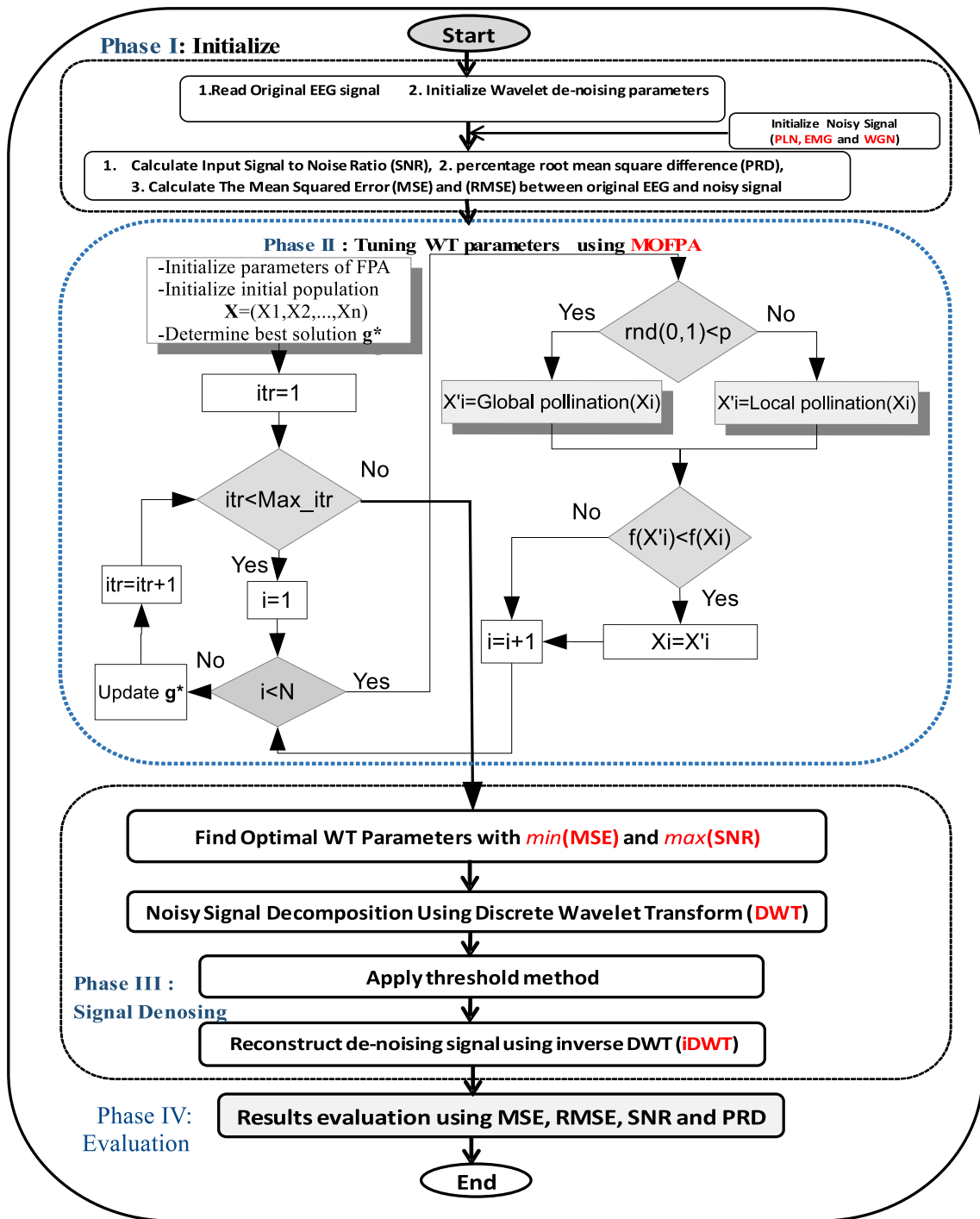
Fig. 3 Proposed method

- EEG signal *decomposition* using DWT. In this step, DWT is applied to decompose the noise of the input EEG signals $x(n)$. The first two Sol'_{opt} parameters, namely MWF ρ and decomposition level L, should be used in the decomposition process. Figure 9a shows the DWT procedure for five levels, where the noisy EEG

signal is divided at each level into cA and cD. The latter is processed using a high-pass filter, whereas the former is processed using a low-pass filter and is decomposed for the next level.

The EEG signal is convolved using the high- and low-pass filters, while the block ($\downarrow 2$), which is represented by the downsampling operator, is used to keep

the even index elements of the EEG signal. The EEG signals are separated into cA and cD based on their frequency and amplitude.

- **Thresholding**. This step is applied based on the noise level of the coefficients. In this step, the last three wavelet parameters, namely thresholding type (β), thresholding selection rules (λ), and re-scaling methods (ρ), must be selected from Sol'_{opt}.

- **Reconstruction of the denoising EEG signal by iDWT**. The value of the original EEG signals $\widehat{X}$ is estimated by applying iDWT on $\widehat{X}$ as follows:

$$z[n] = iDWT[\widehat{X}] \qquad (15)$$

The reconstruction convolves the EEG signals using upsampling ($\uparrow 2$), which involves the insertion of zeros at the even index elements of the EEG signals. Figure 9c shows the iDWT procedure for five levels.

Phase IV: **EEG Denoising Evaluation.** The final phase is evaluating the EEG outcome of WT. The performance of MOFPA-WT is evaluated according to five criteria, namely SNR formulated in Eq. (14), SNR improvement Eq. (16), MSE formulated in Eq. (13), RMSE formulated in Eq. (17), and PRD formulated in Eq. (18).

$$SNR_{imp} = 10 \log_{10} \left\{ \frac{\sum_{n=1}^{N} [\delta(n) - x(n)]^2}{\sum_{n=1}^{N} [x(n) - \widehat{x}(n)]^2} \right\} \quad (16)$$

$$RMSE = \sqrt{\frac{1}{N} \sum_{n=1}^{N} [x(n) - \widehat{x}(n)]^2} \qquad (17)$$

$$PRD = 100 * \sqrt{\frac{\sum_{n=1}^{N} [x(n) - \widehat{x}(n)]^2}{\sum_{n=1}^{N} [x(n)]^2}} \qquad (18)$$

where $x(n)$ denotes the original EEG signal, $\widehat{x}(n)$ is the denoised EEG signal obtained by tuning the wavelet parameters through MOFPA, and N is the number of samples.

6 Results and discussions

The EEG dataset is discussed in Sect. 6.1, the Pareto front evaluation describes in Sect. 6.2, an example to illustrative the behavior of MOFPA-WT in denoising EEG signals is explained in Sect. 6.3, the evaluation of the proposed method is presented in Sect. 6.4, comparative evaluation of MOFPA-WT with state-of-the-arts are given in Sect. 6.5,

and finally comparative evaluation the proposed method with other multi-objective techniques 6.6.

To select the best parameter settings for the proposed method (MOFPA-WT), a sensitivity analysis has been conducted for the switch probability p and population size PoP parameters. The study shows the effect of both parameters using different values such that $p = \{0.0, 0.2, 0.5, 0.8, 1.0\}$ and $PoP = \{10, 20, 50\}$. The analysis study involves all measures which are the MSE, SNR, PRD, RSME, SNR_imp as long as the computation time. As shown from the results recorded in Table 4, the best performance of the (MOFPA-WT) achieved using p=0.8, and PoP=20.

The proposed MOFPA-WT is implementing using MATLAB R2017a on a *LENOVO Ideapad 310, Intel Core i7, RAM 12G*. Table 5 shows the parameter setting of MOFPA-WT method for denoising EEG signals.

In general, the parameter values are selected according to experiments and literature. The switch probability p= 0.8 is selected because it is when the MOFPA achieves the best value for most applications [5, 6]. This is also proved after experimental study shown in the previous section. For the number of iterations, the experiments reveal that no significant improvement is observed for the WT parameters after 100 iterations (see Figs. 13, 14, and 15).

6.1 Datasets

A standard EEG signal dataset, i.e., motor/imagery, is tested on MOFPA-WT[2] [12]. EEG signals from 109 healthy subjects are collated with a brain-computer interface software BCI2000 system [61]. The EEG signals are recorded utilizing 64 fibers (EEG networks), where every antenna is decrypted in a discrete EDF file. Every volunteer conducts multiple motory/imagery tasks that are principally utilized in special disciplines, those of neurological rehabilitation and brain-computer interface applications. In general, these chores comprise of envisaging or simulating a particular action, such as opening and closing the eyelids. The EEG signals are recorded from each volunteer by asking them to perform four tasks depending on the position of the target on the screen. When the target is displayed on the right or right side of the screen, the volunteer must open and close his/her fist, which corresponds with the target position on the screen. The volunteer must open and close his/her fists or feet, if this target appears at the top or bottom of the screen.
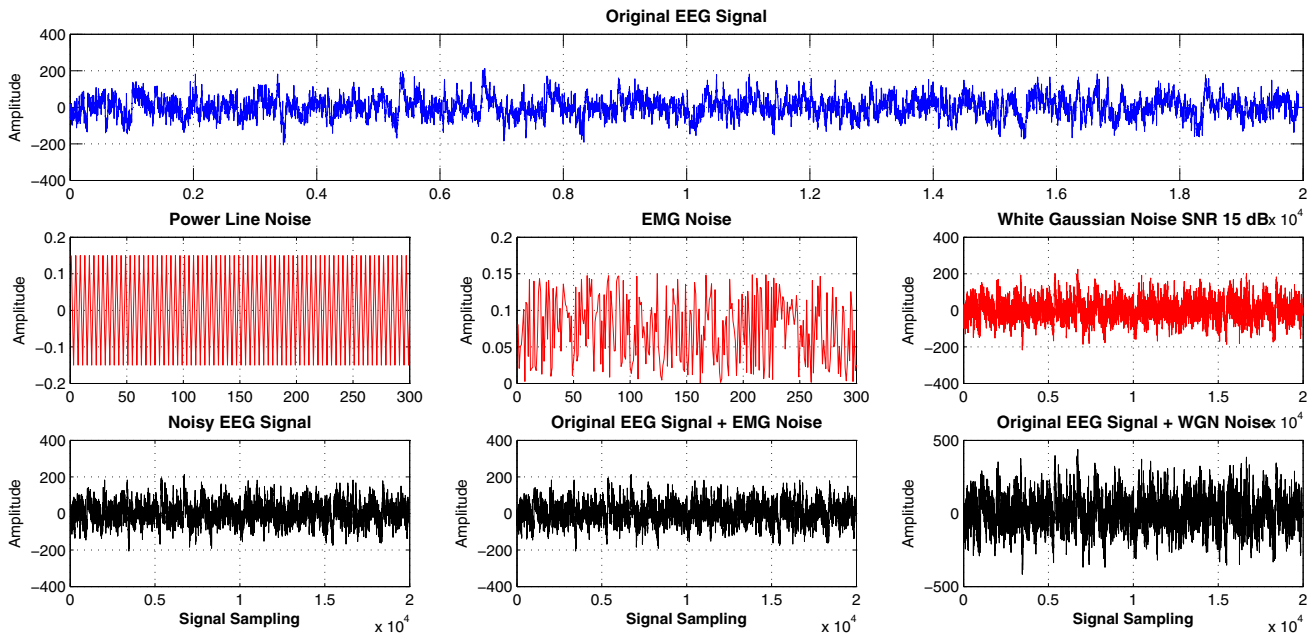
---

[2] https://www.physionet.org/physiobank/database/eegmmidb/.

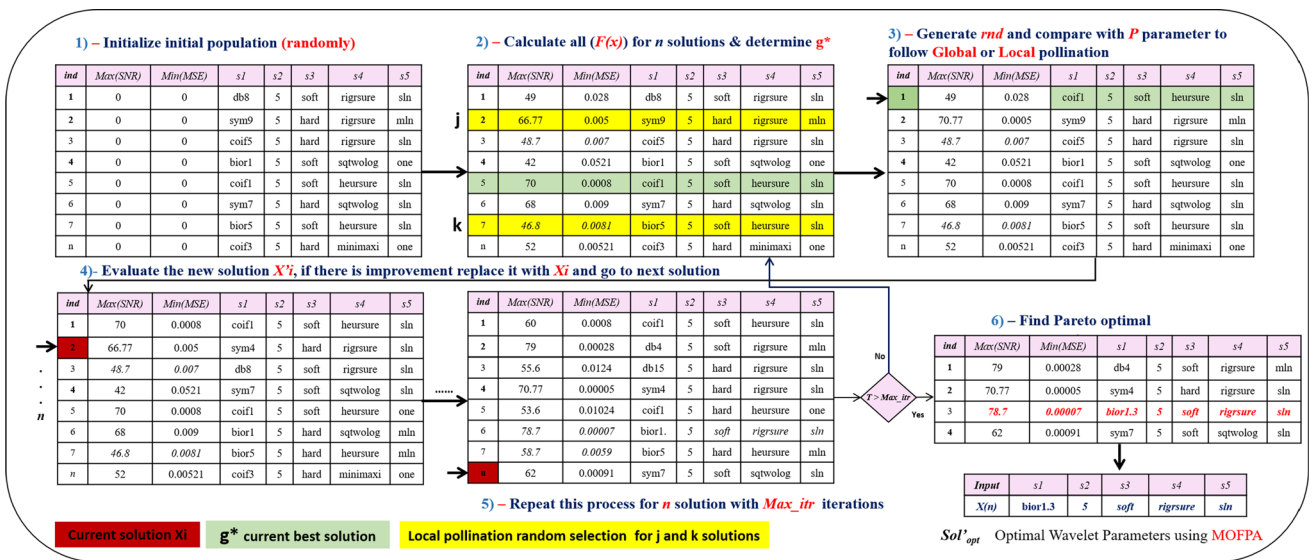**Fig. 4** Original EEG signal corrupted using PLN, EMG, and WGN

Fig. 5 Mechanism of MOFPA for selecting the optimal WT parameters for denoising EEG signals

6.2 Pareto front evaluation

The first evaluation criterion of MOFPA-WT is the Pareto front. According to [5, 62], the Pareto front (PF) can be defined as the set of non-dominated solutions:

$$PF = \{\mathbf{x} \in \mathcal{F} | \nexists \mathbf{x}' \in \mathcal{F} : \mathbf{f}(\mathbf{x}') \prec \mathbf{f}(\mathbf{x})\}, \tag{19}$$

where $\mathcal{F}$ is the feasible search space formed by all feasible solution vector $\mathbf{x}$. A solution $\mathbf{x}$ is said to dominate another solution $\mathbf{x}'$ if and only if $x_i \leq x_i'$ for $\forall i \in \{1, 2, ..., D\}$ in the

D-dimensional space. This dominance relationship can be written compactly as

$$\mathbf{x} \prec \mathbf{x}'. \tag{20}$$

In addition, $\mathbf{f} = (f_1, f_2)$ corresponds to the two objectives shown in Fig. 6, where f_1 and f_2 refers to mean squared error (MSE) (Eq. 13) and signal-to-noise ratio (SNR) (Eq. 14), respectively.

Figures 6, 7, and 8 show the Pareto fronts and MOFPA-WT for the three different EEG noise which are PLN,

ENG, and WGN, respectively. As aforementioned, we have two objectives functions: f_1 represents the *MSE* and f_2 refers to SNR. The blue points in these figures represent the Pareto fronts which are a set of non-dominated solutions to the denoising process. The plotting curve shows that there are impacted trade-offs between f_1 and f_2. While the red points represent the selected solutions achieved by the MOFPA-WT. Note that the selected solution is chosen based on domination criterion wherein the "min MSE" and "max SNR" are improved. The sub-figures in Figs. 6 and 7 represent the magnified portion of the original figure to show the performance of the MOFPA-WT for EEG signal denoising in specific point.

To elaborate the discussion about the performance of the proposed MOFPA-WT for EEG signal denoising, the effects of PLN and EMG noise shown in Figs. 6 and 7 are emphasized in which the denoising performance has highly influenced where it is always close to the top-left corner. This means that the MOFPA-WT is always providing higher signal-to-noise ratios. On the other hand, in Fig. 8, the MOFPA-WT obtained a sparse values and distributed along Pareto fronts approx. This can be noticed by the results achieved for WGN noise because the input EEG signal has been corrupted with a large amount of noise. For that, the proposed MOFPA-WT tried to select the dominant solutions where these solutions should have "min MSE" and "max SNR".

6.3 Illustrative example

To explain further the behavior of MOFPA-WT in denoising EEG signals, EEG signal $x(n)$ is supposed to have been denoised using MOFPA-WT. As mentioned in the above section and in accordance with the example in Fig. 5, MOFPA-WT involves four phases. In Phase I (*initialization*), the input EEG signal $x(n)$ is corrupted with three noises types of noise, namely WGN, PLN, and EMG, as shown in Eqs. (6), (8), and (10), respectively. The SNR, MSE, RMSE, and PRD of $x(n)$ are computed for the noised EEG signal $x(n)$, as shown in Eqs. (14), (13), (17), and (18), respectively. Meanwhile, the MOFPA parameters are initialized as follows: switch probability $(p)= 0.8$, maximum number of iterations $(Max_{itr})= 100$, population size$= 20$, and dimension of the search variables $(d)= 5$.

In Phase II (*tuning wavelet denoising parameters by MOFPA*), MOFPA finds the optimal solution of the WT parameters Sol'_{opt} to address the EEG signal denoising problem. For example, let the solutions in the MOFPA population be given as shown in Fig. 5. Table 6 shows how the MOFPA iteration loops to improve the WT parameters until Sol'_{opt}, which contains the optimal parameter values to be used by WT, is obtained. In Iteration 1, MOFPA

determines $Sol'_{opt}(1)$ from the initial population, where $f(MOFPAWT)(1) = 22.2975$. In Iteration 2, $Sol'_{opt}(2)$ with $f(x(2)) = 98.3952$ is generated. Notably, the Sol'_{opt} dose not replace the previous $Sol'_{opt})(1)$ because the current solution is worse than the previous solution. MOFPA continues to look for an optimal solution. In Iteration 8, MOFPA produces $Sol'_{opt}(8)$ with $f(MOFPAWT(8) = 0.0075$. The best solution Sol'_{opt} will replace the previous $Sol'_{opt}(1)$. According to Table 6, the next improvement of Sol'_{opt} is achieved at Iteration 14 where $f(MOFPAWT)(14) = 0.0075$ and the best solution Sol'_{opt} will be replaced by $Sol'_{opt}(8)$. Thereafter, nothing changes until the last iteration is reached. The optimal parameter setting for WT is given by $Sol'_{opt}(100)$. The Sol'_{opt} solution obtained by MOFPA in this example is shown in Fig. 7. Sol'_{opt} solution will be passed onto the next phase.

Phase III (*EEG denoising using WT with Sol'_{opt}*) involves three steps, namely EEG signal *decomposition* using DWT, *thresholding* and *reconstruction*. Figure 9 shows the EEG denoising process. In the *decomposition* step, the noisy EEG signal is decomposed using MWF $\rho = bior1.3$ and decomposition level $L= 5$ while the EEG signal is divided into five levels based on the value of L. Each level is filtered separately using the wavelet function $\rho = bior1.3$ to obtain a smooth EEG signal. Fig. 9 shows the decomposition process. In *Thresholding*, the threshold value δ is defined based on the noisy coefficients of each level, and each cD is processed using Sol'_{opt} parameters. The Sol'_{opt} for thresholding has the following parameters: thresholding type $(\beta) = soft$, selection rules $(\lambda) = rigrsure$, and rescaling methods $(\rho) = sln$. The denoised EEG signal is then reconstructed using iDWT. Figure 9c shows the reconstruction of an EEG signal with five decomposition levels.

Suppose there is an EEG signal and we need to denoise it using wavelet denoising method with the following parameters MWF $\rho = bior1.3$, decomposition level $L= 5$, thresholding type $(\beta) = soft$, selection rules $(\lambda) = rigrsure$, and rescaling methods $(\rho) = sln$. Therefore, in the *decomposition* phase, the EEG signal is decomposed using MWF $\rho = bior1.3$ and decomposition level $L= 5$ while the EEG signal is divided into five levels based on the value of L. Each level is filtered separately using the wavelet function $\rho = bior1.3$ to obtain a smooth EEG signal. Figure 10 shows the decomposition process. In *Thresholding*, the threshold value δ is defined based on the noisy coefficients of each level, and each cD is processed using wavelet denoising parameters. As mentioned above, the wavelet

---

2 https://www.physionet.org/physiobank/database/eegmmidb/.

Table 4 Sensitivity analysis of MOFPA-WT to its p and population size PoP parameters for PLN noises for motor imaging EEG dataset

Population_Size	p value of FPA	MSE	RMSE	PRD	SNR	SNR_imp	Time	Noise_type
	$p = 0$	0.0113	0.1061	0.1928	54.2996	17.3480	27.2236	
	$p = 0.2$	0.0112	0.1060	0.1926	54.3068	17.3485	21.5744	
PoP=10	$p = 0.5$	0.0112	0.1061	0.1927	54.3023	17.3482	21.9967	PLN
	$p = 0.8$	0.0112	0.1060	0.1926	54.3052	17.3484	26.5080	
	$p = 1$	0.5174	0.7193	1.3069	37.6754	15.7606	24.2744	
Population_Size	p value of FPA	MSE	RMSE	PRD	SNR	SNR_imp	Time	Noise_type
	$p = 0$	0.0112	0.1060	0.1926	54.3081	17.3486	47.7417	
	$p = 0.2$	0.0112	0.1060	0.1926	54.3055	17.3484	41.1825	
PoP=20	$p = 0.5$	0.0112	0.1060	0.1926	54.3068	17.3485	41.1996	PLN
	$p = 0.8$	**0.0111**	**0.1054**	**0.1890**	**54.4694**	**17.3615**	**40.7875**	
	$p = 1$	0.7081	0.8415	1.5289	36.3124	15.6005	67.3693	
Population_Size	p value of FPA	MSE	RMSE	PRD	SNR	SNR_imp	Time	Noise_type
	$p = 0$	0.0112	0.1060	0.1926	54.3081	17.3486	112.8156	
	$p = 0.2$	0.0112	0.1060	0.1926	54.3081	17.3486	129.6190	
PoP=50	$p = 0.5$	0.0112	0.1060	0.1926	54.3068	17.3485	97.6566	PLN
	$p = 0.8$	0.0112	0.1060	0.1927	54.3042	17.3483	117.8875	
	$p = 1$	0.0133	0.1153	0.2095	53.5762	17.2897	183.2313	

Values in bold indicate the best solution achieved

Table 5 Parameters setting for MOFPA

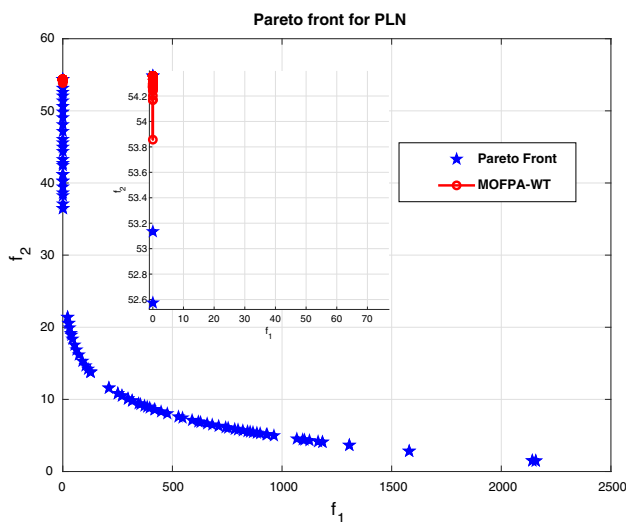| FPA parameters	MOFPA
Switch probability (p)	0.8
No. of iterations	100
Population size PoP	20
Dimension of search variables (d)	5

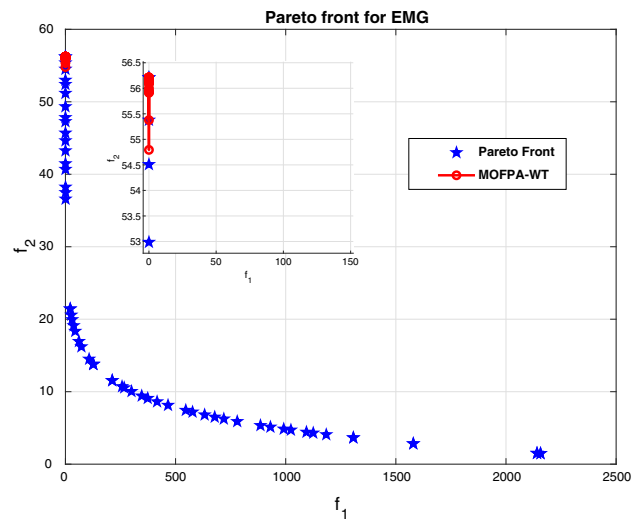**Fig. 6** Comparison results of Pareto front and MOFPA-WT for PLN noises

Fig. 7 Comparison results of Pareto front and MOFPA-WT for EMG noises

denoising for thresholding has the following parameters: thresholding type (β) = *soft*, selection rules (λ) = *rigrsure*, and rescaling methods (ρ) = *sln*. Figure 11 shows the application of thresholding for denoising EEG signals with five decomposition levels (i.e., d1, d2, d3, d4, and d5) based on the value of wavelet denoising parameters. The *dotted blue line* in Fig. 11 represents the thresholding value δ for each level. The denoised EEG signal is then reconstructed using iDWT.
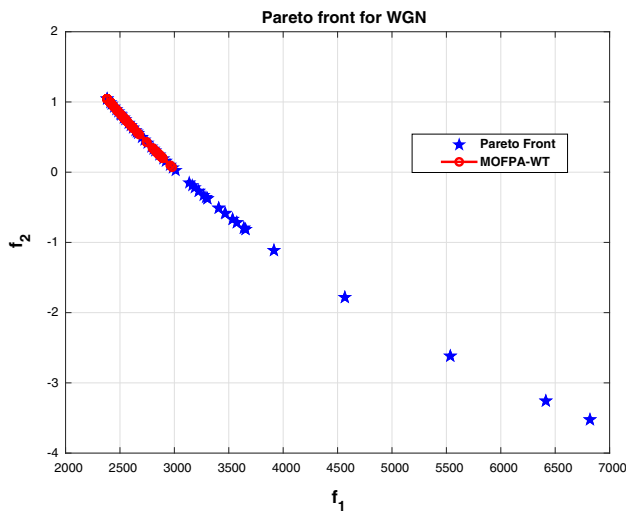
Fig. 8 Comparison results of Pareto front and MOFPA-WT for WGN noises

6.4 Evaluation of multi-objective functions in MOFPA-WT

The second experiment is conducted to show the effect of the Multi-objective functions on the performance of MOFPA-WT. Three versions of FPA-based WT are designed to evaluate the proposed multi-objective function in MOFPA-WT. The first is the proposed MOFPA-WT, which combines MSE and SNR as a multi-objective function, to find the optimal parameter setting for WT. The second is FPA with only MSE to find the optimal parameter settings for WT (i.e., FPA-MSE-WT). The third is FPA with only SNR to find the optimal parameter setting for WT (i.e., FPA-SNR-WT).

Five measures, namely SNR, SNR improvement, MSE, RMSE, and PRD, are used to evaluate the EEG signal quality, which is denoised by using the proposed MOFPA-WT. Table 8 shows the optimal WT parameters for EEG signals denoising achieved by MOFPA-WT, FPA-SNR-WT, and FPA-MSE-WT, and Table 9 shows the performance of these three methods according to PLN, EMG, and WGN noises for EEG motor movement/imaging dataset. The quality of the final outcomes of the denoised EEG signal using MOFPA-WT, FPA-SNR-WT, and FPA-MSE-WT are compared. Figure 12 shows the evaluation results of the denoising of EEG signals according to the five measures. MOFPA-WT achieves the best results for EEG signal denoising with different noises compared with FPA-SNR-WT and FPA-MSE-WT. Conversely, FPA-SNR-WT and FPA-MSE-WT shows deformation of the EEG signal

in some cases, such as with EMG and WGN noises. For the PLN, the proposed MOFPA-WT achieves the highest SNR (54.3575) and SNR improvement (0.0555); meanwhile, where the other two techniques cannot preserve or improve the SNR value, in which FPA-MSE-WT and FPA-SNR-WT achieve -0.0397 and 0, respectively. For the EMG noise, the proposed method also achieves the highest SNR improvement (0.0116), whereas the SNR improvement for FPA-MSE-WT and FPA-SNR-WT is -0.0240 and 0, respectively. For high amount of noise, such as in WGN, MOFPA-WT obtains an SNR improvement of 1.1947, whereas those of FPA-SNR-WT and FPA-MSE-WT are 0 and 0.6180, respectively.

Also, the results of MOFPA-WT are evaluated using Wilcoxon signed-rank statistical test [63] to determine the significance of MOFPA-WT for EEG signal denoising compared with the other methods. Table 10 shows the pairwise comparison between the MOFPA-WT and other methods (FPA-MSE-WT and FPA-SNR-WT). The proposed MOFPA-WT shows significant results for all EEG datasets used.

The MOFPA-WT is tested using different noise types, namely PLN, EMG, and WGN. Figs. 13, 14, and 15 show the efficient performance of MOFPA-WT, especially with PLN and EMG noises, where achieving the optimal solution at around 5 and 13 iterations, respectively, is possible; however, more than 90 iterations are needed to obtain the optimal WT parameters for WGN noise.

6.5 Comparative evaluation MOFPA-WT with other multi-Objective techniques

Initially, the performance of the MOFPA-WT is compared with two popular multi-objective methods such as NSGA-II [64] and MOPSO [65]. The power line noise (PLN) was used to evaluate the performance of the proposed method (MOFPA-WT) with selected popular techniques. The parameters of NSGA-II used in the experiments are population size $PoP = 50$, crossover $= 0.5$, mutation $= 0.5$, $itr = 100$. Also, the parameters of MOPSO used in the experiments are population size $PoP = 50$, accelerate constant $c1 = 2$, $c2 = 2$, maximum and minimum velocity $vmax = 0.9$, $vmin = 0.1$, and total number of iteration $itr = 100$. These values are carefully selected such as used in [64] and [65]. Compared with NSGA-II [64] and MOPSO [65], MOFPA-WT produces better results and Table (11) shows comparative results using 5 measures,

Table 6 Some recorded iterations using MOFPA to achieve optimal WT parameters

Iteration	s1	s2	s3	s4	s5	$f(_{\text{MOFPAWT}})$	Decision
1	db10	Five	Hard(h)	Rigrsure	One	22.2975	Best $Sol'_{\text{opt}}(1)$
2	bior3.1	Five	Hard(h)	Heursure	One	98.3952	Do not replace $Sol'_{\text{opt}}(1)$
3	db43	Five	Hard(h)	Heursure	sln	34.5718	Do not replace $Sol'_{\text{opt}}(1)$
4	db10	Five	Hard(h)	Heursure	One	34.7521	Do not replace $Sol'_{\text{opt}}(1)$
5	db13	Five	Hard(h)	Heursure	sln	34.5416	Do not replace $Sol'_{\text{opt}}(1)$
6	bior3.9	Five	Hard(h)	Heursure	One	38.9375	Do not replace $Sol'_{\text{opt}}(1)$
7	bior3.7	Five	Hard(h)	Rigrsure	One	37.6392	Do not replace $Sol'_{\text{opt}}(1)$
8	bior2.2	Five	Hard(h)	Heursure	One	**0.0075**	**Replace the best** $Sol'_{\text{opt}}(8)$
10	bior2.2	Five	Hard(h)	Heursure	One	**0.0075**	Nothing changes in. $Sol'_{\text{opt}}(8)$
11	db18	Five	Hard(h)	Heursure	One	33.1429	Do not replace $Sol'_{\text{opt}}(8)$
12	db10	Five	Hard(h)	Heursure	One	33.1429	Do not replace $Sol'_{\text{opt}}(8)$
13	sym5	Five	Hard(h)	Rigrsure	One	33.1647	Do not replace $Sol'_{\text{opt}}(8)$
14	bior1.3	Five	Soft(s)	Rigrsure	sln	**0.0074**	**Replace the best** $Sol'_{\text{opt}}(14)$
20	bior1.3	Five	Soft(s)	Rigrsure	sln	**0.0074**	Nothing changes in. $Sol'_{\text{opt}}(14)$
90	bior1.3	Five	Soft(s)	Rigrsure	sln	**0.0074**	Nothing changes in. $Sol'_{\text{opt}}(14)$
100	bior1.3	Five	Soft(s)	Rigrsure	sln	**0.0074**	Nothing changes in. $Sol'_{\text{opt}}(14)$

Values in bold indicate the best solution achieved

Table 7 Sol'_{opt} WT parameters for EEG denoising

Input Signal	S1	S2	S3	S4	S5
$X(n)$	bior1.3	5	Soft	Rigrsure	Sln

MSE, RMSE, PRD, SNR and SNR_imp. Moreover, MOFPA-WT, MOGA-WT and MOPSO-WT convergence rates are presented in which the suggested method (MOFPA-WT) provides faster archives than MOGA-WT and MOPSO-WT, for the best solution. Figure 16 shows
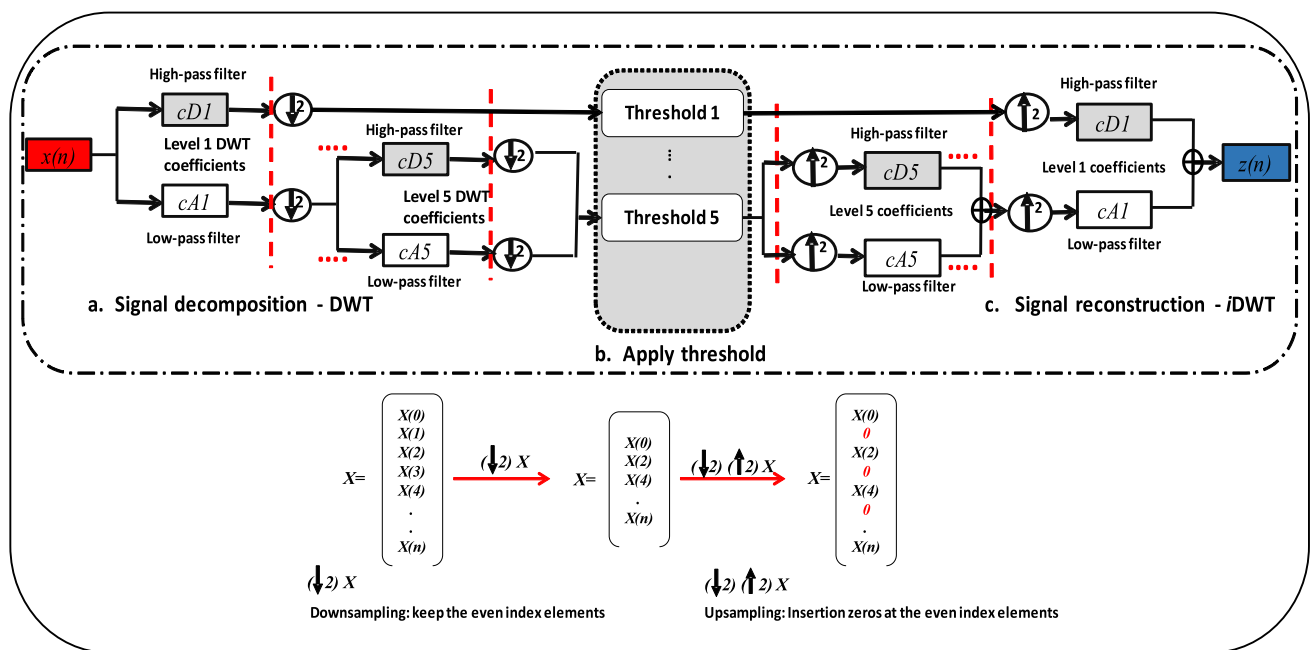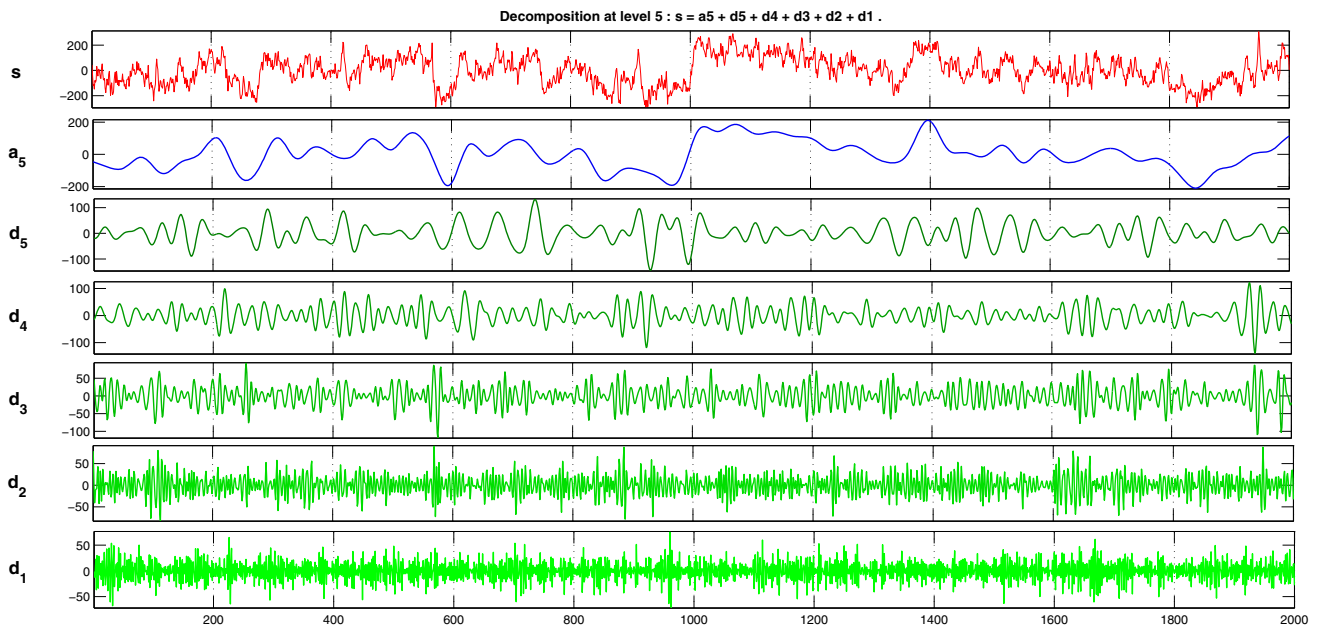

Fig. 9 EEG denoising process

Fig. 10 EEG Decomposition process for five levels

the comparison results of MOFPA-WT with NSGA-II [64] and MOPSO [65] using PLN noises.

Table 11 summarized the results of 100 repetitions. To further evaluate the results of MOFPA-WT compared with

NSGA-II [64] and MOPSO [65]. T-test is conducted based on mean to determine the significance of MOFPAWT for EEG signal denoising. Table 12 shows the pair-wise comparison between the MOFPA-WT and other methods (NSGA-II-WT and MOPSO-WT). The proposed method
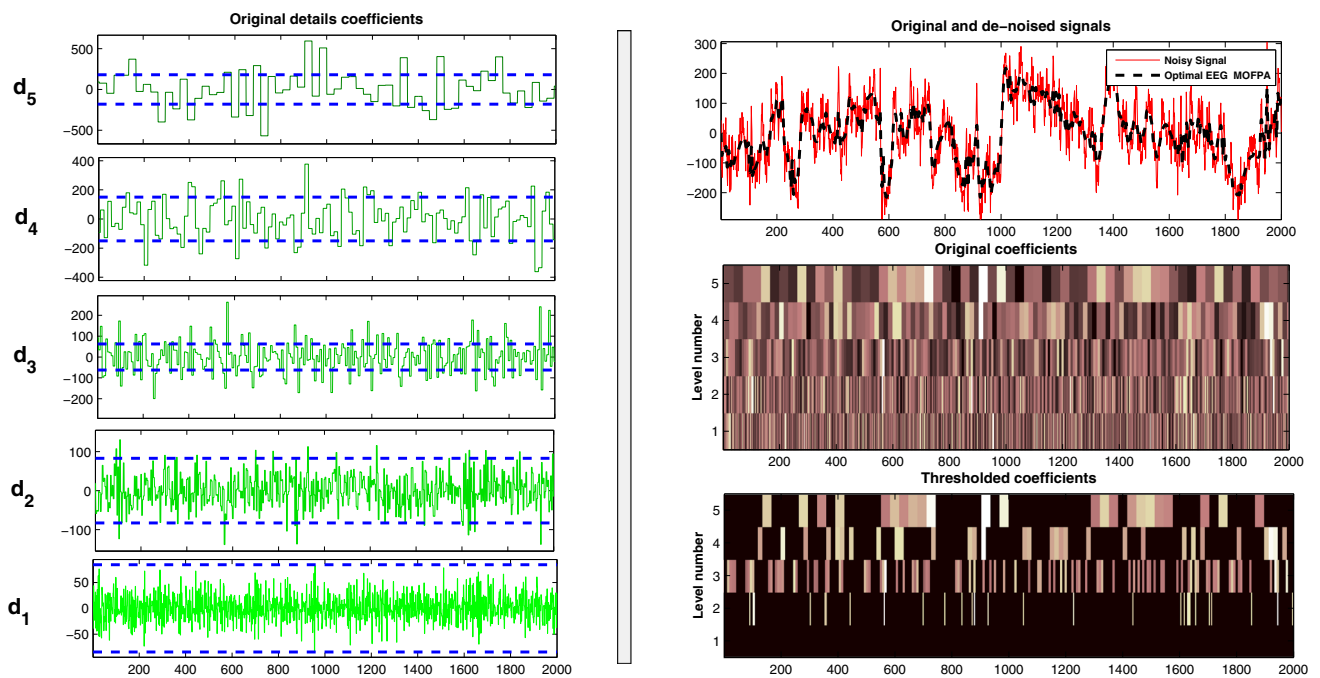

Fig. 11 Thresholding and Reconstruction steps

Table 8 Optimal WT parameters obtained by FPA-SNR-WT, MOFPA-WT, FPA-MSE-WT for PLN, EMG, and WGN noises for motor imaging EEG dataset

Algorithm	Noise	W.Rescaling	Thr. Sel	Thr. type	Decom. Level	Wavelet Fun.
FPA-SNR-WT	PLN	Rigrsure	Hard	One	5	db45
MOFPA-WT	**PLN**	**Rigrsure**	**Hard**	**One**	**5**	**bior1.5**
FPA-MSE-WT	PLN	Rigrsure	Hard	One	5	coif3
FPA-SNR-WT	EMG	Rigrsure	Hard	One	5	sym2
MOFPA-WT	**EMG**	**Rigrsure**	**Hard**	**One**	**5**	**bior1.3**
FPA-MSE-WT	EMG	Rigrsure	Hard	One	5	db13
FPA-SNR-WT	WGN	Heursure	Hard	mln	5	db24
MOFPA-WT	**WGN**	**Rigrsure**	**soft**	**mln**	**5**	**coif5**
FPA-MSE-WT	WGN	Rigrsure	soft	sln	5	db31

Values in bold indicate the best solution achieved

Table 9 Performance of MOFPA in denoising EEG signals according to PLN, EMG, and WGN for EEG motor imaging dataset

Method	Noise	SNR_{out}(dB)	SNR_{imp} (dB)	PRD	MSE	RMSE
FPA-SNR-WT	PLN	54.3021	0	0.1927	0.0113	0.1061
MOFPA-WT	**PLN**	**54.3575**	**0.0555**	**0.191**	**0.0111**	**0.1054**
FPA-MSE-WT	PLN	54.2624	−0.0397	0.1920	**0.0111**	**0.1054**
FPA-SNR-WT	EMG	56.195	0	0.155	0.0073	0.0853
MOFPA-WT	**EMG**	**56.2067**	**0.0116**	**0.1547**	0.0072	0.0851
FPA-MSE-WT	EMG	56.1710	−0.0240	0.1554	**0.0071**	**0.0843**
FPA-SNR-WT	WGN	−0.1502	0	101.7451	3.14E+03	56.0005
MOFPA-WT	**WGN**	**1.0444**	**1.1947**	**88.6702**	**2.38E+03**	**48.804**
FPA-MSE-WT	WGN	0.4677	0.6180	94.7577	**2.38E+03**	**48.804**

Values in bold indicate the best results; for SNR and SNRimp, the highest value is the best, whereas for MSE, RMSE, and PRD, the lowest value is the best
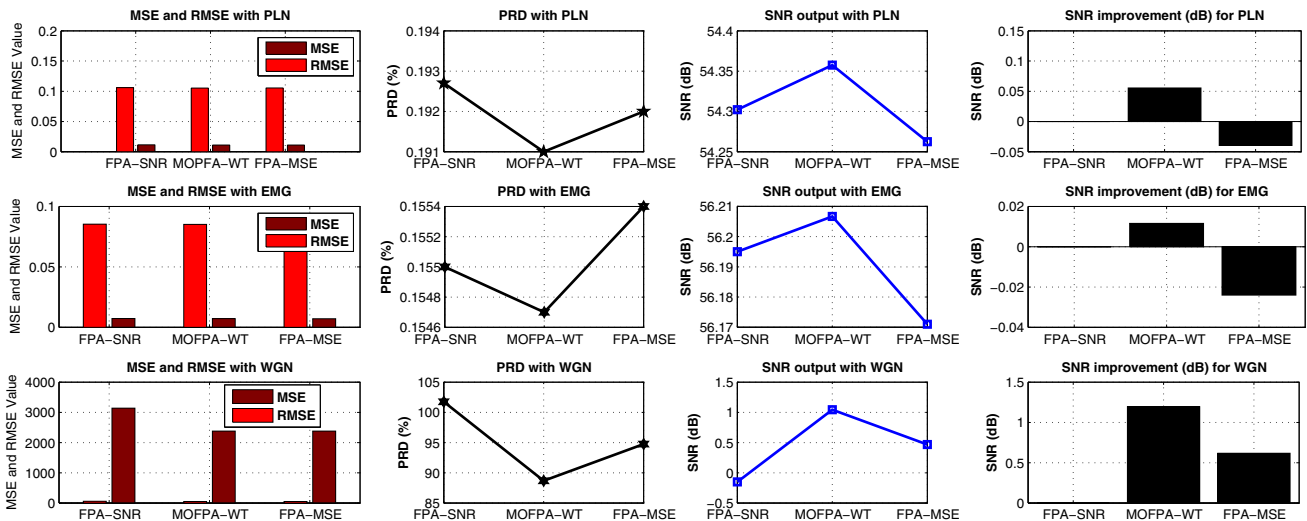

Fig. 12 Comparison results of FPA-SNR, MOFPA-WT, and FPA-MSE for EMG, PLN, and WGN noises

Table 10 Wilcoxon signed-rank test evaluation

Method	MOFPA-WT with FPA-MSE-WT			MOFPA-WT with FPA-SNR-WT		
	Mean difference	P_{value}	Significant	Mean difference	P_{value}	Significant
Noise$_{PLN}$	0	**0.00512**	+	0.06	**0.00512**	+
Noise$_{EMG}$	0	**0.00512**	+	0.01	**0.00512**	+
Noise$_{WGN}$	−6.09	**0.00512**	+	1.19	**0.00512**	+

+ values in bold indicate significant, − indicates no significant
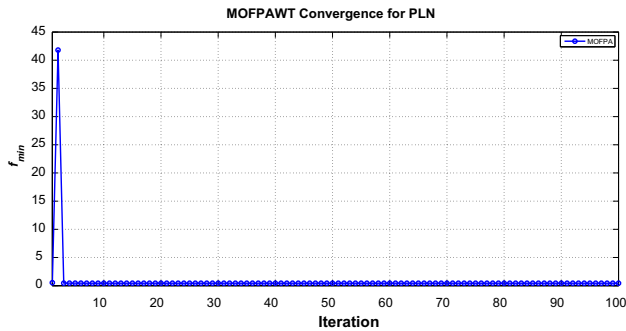
Fig. 13 Convergence results of PLN
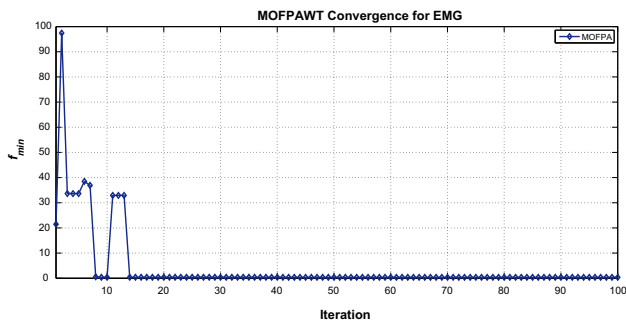
Fig. 14 Convergence results of EMG
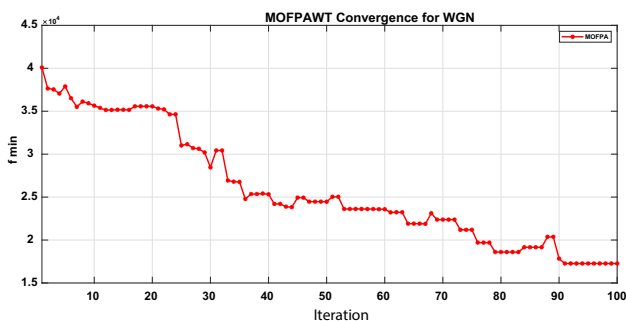
Fig. 15 Convergence results of WGN

(MOFPA-WT) shows significant results compared with both methods.

6.6 Comparing the MOFPA-WT with state-of-the-art methods

The MOFPA-WT is compared to four advanced EEG signal denoising proposed by Al-Qazzaz et al. [28], Kumari et al. [13], Bhatnagar et al. [66], and Al-Salman et al. [67]. The comparison is carried out on the basis of standard data sets, i.e., motor/imaging [12], with PLN and EMG corrupt in their original EEG signal [59, 60]. Five criteria, i.e., MSE, RMSE, SNR_{imp}, and PRD, are used to assess the final outcome. Table 13 describes the performance of MOFPA-WT and these methods. Apparently, the proposed approach (MOFPA-WT) achieves the best results in comparison with other methods for every comparative measures.

7 Conclusion and future work

A novel technique for EEG signal denoising problem based on MOFPA-WT is proposed in this study. The most successful denoising technique in the signal processing domain is wavelet transform (WT). The success of WT is based on the configurations of its five parameters (i.e., (i) MWF Φ, (ii) decomposition level L, (iii) thresholding function β, (iv) threshold selection rule λ, and (v) threshold re-scaling method ρ). The configuration of the WT parameter is critical and accomplished based on user experience. In this study, the problem is modeled as a multi-objective function based on minimum mean squared error (MSE) and maximum signal-to-noise-ratio (SNR). The optimization method called FPA is used with the multi-objective function to set the optimal WT parameter, thereby improving the EEG signal denoising results.

MOFPA-WT is evaluated using a standard EEG dataset, namely the EEG motor movement/imagery dataset. This dataset contains data of 109 volunteers, and EEG signals are captured from 64 EEG channels based on different

Fig. 16 Comparison results of MOFPA-WT with other multi-objective techniques using PLN noises
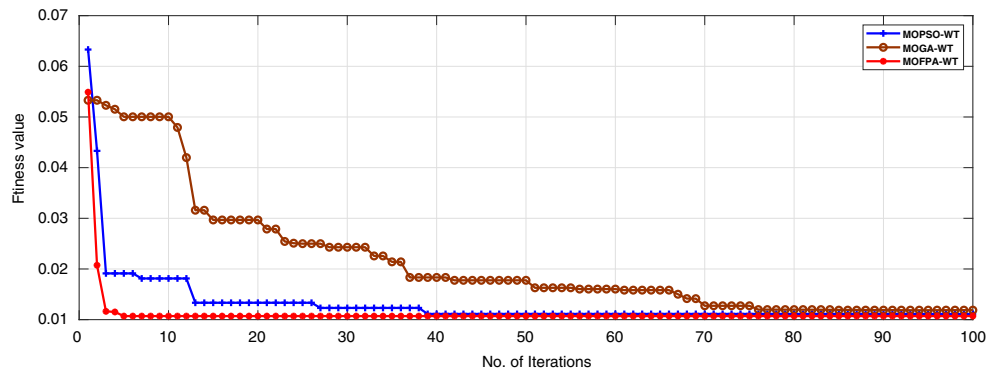

Table 11 Comparative evaluation MOFPA-WT with NSGA-II (MOGA-WT) and MOPSO (MOPSO-WT)

Method	Measures	MSE	RMSE	PRD	SNR	SNR_imp
	Best	**0.0112**	0.1060	**0.1927**	**54.3042**	**17.3483**
	Worst	**0.0113**	**0.1061**	**0.2031**	**53.8446**	**17.3114**
MOFPA-WT	Mean	**0.0113**	**0.1061**	**0.2031**	**53.8462**	**17.3116**
	Std	**0.0000**	**0.0000**	**0.0000**	**0.0014**	**0.0001**
	Median	**0.0113**	**0.1061**	**0.2031**	**53.8457**	**17.3115**
	Best	**0.0112**	**0.1058**	0.2026	53.8669	17.3132
	Worst	1.1095	1.0533	2.0168	33.9067	15.3029
MOPSO-WT	Mean	0.0735	0.1728	0.3309	52.1210	17.1442
	Std	0.2185	0.2125	0.4068	5.2063	0.5089
	Median	**0.0113**	0.1062	0.2033	53.8370	17.3108
	Best	0.0113	0.1062	0.2034	53.8313	17.3104
	Worst	1.3403	1.1577	2.2167	33.0860	15.1964
MOGA-WT	Mean	0.5128	0.5771	1.1050	42.6655	16.2130
	Std	0.5283	0.4314	0.8261	8.7565	0.8864
	Median	0.3341	0.5780	1.1068	39.1189	15.9239

Bold value indicates best results where for SNR, SNRimp, highest is best and for MSE, RMSE, and PRD, lowest is best

Table 12 T-test evaluation

Method	Mean	*p*-value	*t*-value	Result
MOFPA-WT with NSGA-II	0.01	0.00001	9.11	++
MOFPA-WT with MOPSO	0.0	0.00001	6.15	++

++ means there is a significant, and – means there is not significant

mental tasks. These EEG signals are corrupted using three different noises, namely PLN, EMG, and WGN [26, 59, 60]. Five evaluation criteria are used, namely SNR, SNR improvement, MSE, RMSE, and PRD. To show the effect of the multi-objective aspects on the performance of the proposed MOFPA-WT, the behavior of FPA for EEG signal denoising is tested using FPA with MSE, FPA with SNR, and FPA with MSE and SNR. The experiments show that MOFPA-WT can provide more subjective results than the other two. The convergence rate and Pareto front are also studied for the proposed MOFPA-WT.

For future work, one of the possible works is to apply independent component analysis (ICA) [68], e.g., before apply the proposed method (MOFPA-WT) to achieve better results for EEG signal denoising. Also, MOFPA-WT will be applied for more challenging signal problem instances, such as person authentication or early detection of epilepsy based on EEG signal. Furthermore, the real-world applications are required to show the efficiency of MOFPA-WT.

Table 13 Comparing the proposed MOFPA-WT method with state-of-the-art methods for EEG signals denoising with different noises

Power Line Noise (PLN)

Method/Measures	MSE	RMSE	PRD	SNR	SNR_imp	Decom. Level	Wavelet Fun.	W.Rescaling	Thr. Sel	Thr. type
Proposed method (MOFPA-WT)	**0.0111**	**0.1054**	**0.189**	**54.4694**	**17.3615**	L=5	bior1.5	Rigrsure	Hard	One
Kumari et al. [13]	0.0113	0.1061	0.1903	54.4124	17.357	L=5	db4	Rigrsure	Hard	One
Al-Qazzaz et al. [28]	0.0197	0.1402	0.2515	51.9907	17.1593	L=5	sym9	Rigrsure	Hard	One
Bhatnagar et al. [66]	0.0222	0.1489	0.2671	51.4678	17.1154	L=4	db1	Rigrsure	Soft	One
Al-Salman et al. [67]	0.0152	0.1231	0.2208	53.119	17.2525	L=3	db6	Rigrsure	Hard	One

EMG Noise

Method/Measures	MSE	RMSE	PRD	SNR	SNR_imp	Decom. Level	Wavelet Fun.	W.Rescaling	Thr. Sel	Thr. type
Proposed method (MOFPA-WT)	**0.0074**	**0.0862**	**0.1547**	**56.2115**	**17.4983**	L=5	bior1.3	Rigrsure	Hard	One
Kumari et al. [13]	0.0075	0.0866	0.1549	55.3251	17.1332	L=5	db4	Rigrsure	Hard	One
Al-Qazzaz et al. [28]	**0.0074**	0.0863	**0.1547**	56.2081	17.498	L=5	sym9	Rigrsure	Hard	One
Bhatnagar et al. [66]	0.0127	0.1126	0.202	53.8945	17.3154	L=4	db1	Rigrsure	Soft	One
Al-Salman et al. [67]	**0.0074**	**0.0862**	**0.1547**	56.2114	17.4982	L=3	db6	Rigrsure	Hard	One

Bold font highlights the best obtained results. Note that for SNR and SNRimp, the highest value is the best and for MSE, RMSE, and PRD, the lowest is the best

Declarations

Conflict of interest The authors declare that they have no conflict of interest.

References

1. Alyasseri ZAA, Khader AT, Al-Betar MA (2017) Optimal electroencephalogram signals denoising using hybrid β-hill climbing algorithm and wavelet transform. In: Proceedings of the international conference on imaging, signal processing and communication, pp 106–112
2. Yang XS (2012) Flower pollination algorithm for global optimization. In: International conference on unconventional computing and natural computation, Springer, pp 240–249
3. Alyasseri ZAA, Khader AT, Al-Betar MA, Awadallah MA, Yang XS (2018) Variants of the flower pollination algorithm: a review. In: Nature-inspired algorithms and applied optimization, Springer, pp 91–118
4. Al-Betar MA, Awadallah MA, Doush IA, Hammouri AI, Mafarja M, Alyasseri ZAA (2019) Island flower pollination algorithm for global optimization. J Supercomput 75(8):5280–5323
5. Yang X-S, Karamanoglu M, He X (2013) Multi-objective flower algorithm for optimization. Proc Comput Sci 18:861–868
6. Yang X-S, Karamanoglu M, He X (2014) Flower pollination algorithm: a novel approach for multiobjective optimization. Eng Opt 46(9):1222–1237
7. Tamilselvan V, Jayabarathi T (2016) Multi objective flower pollination algorithm for solving capacitor placement in radial distribution system using data structure load flow analysis. Arch Electrical Eng 65(2):203–220
8. Azis MF, Ryanta A, Putra DFU, Fenno O (2015) Dynamic economic dispatch considering emission using multi-objective flower pollination algorithm. In: ASEAN/Asian Academic Society international conference proceeding series
9. Shilaja C, Ravi K (2017) Multi-objective optimal power flow problem using enhanced flower pollination algorithm. Gazi Univ J Sci 30(1):79–91
10. Rajaram R, Kumar KS (2015) Multiobjective power loss reduction using flower pollination algorithm. Int J Control Theory Appl 8(5):2239–2245
11. Rajalashmi K, Prabha S (2017) A hybrid algorithm for multiobjective optimal power flow problem using particle swarm algorithm and enhanced flower pollination algorithm. Asian J Res Soc Sci Humanities 7(1):923–940
12. Goldberger AL, Amaral LA, Glass L, Hausdorff JM, Ivanov PC, Mark RG, Mietus JE, Moody GB, Peng C-K, Stanley HE (2000) Physiobank, physiotoolkit, and physionet. Circulation 101(23):e215–e220
13. Kumari P, Vaish A (2015) Brainwave based user identification system: a pilot study in robotics environment. Robot Auto Syst 65:15–23
14. Sharma PK, Vaish A (2016) Individual identification based on neuro-signal using motor movement and imaginary cognitive process. Optik Int J Light Electron Opt 127(4):2143–2148
15. Alyasseri ZAA, Khader AT, Al-Betar MA, Alomari OA (2020) Person identification using eeg channel selection with hybrid flower pollination algorithm. Pattern Recogn, 107393
16. Ramadan RA, Vasilakos AV (2017) Brain computer interface: control signals review. Neurocomputing 223:26–44
17. Alyasseri ZAA, Khadeer AT, Al-Betar MA, Abasi A, Makhadmeh S, Ali NS (2019) The effects of EEG feature extraction using multi-wavelet decomposition for mental tasks classification. In: Proceedings of the international conference on information and communication technology, pp 139–146
18. Rao RP (2013) Brain-computer interfacing: an introduction. Cambridge University Press, Cambridge
19. Berger H (1929) Über das elektrenkephalogramm des menschen. Eur Arch Psychiatry Clin Neurosci 87(1):527–570

20. Abdulkader SN, Atia A, Mostafa M-SM (2015) Brain computer interfacing: applications and challenges. Egypt Inf J 16(2):213–230

21. Prabhakar SK, Rajaguru H, Lee S-W (2020) A framework for schizophrenia eeg signal classification with nature inspired optimization algorithms. IEEE Access 8:39875–39897

22. Souri A, Ghafour MY, Ahmed AM, Safara F, Yamini A, Hoseyninezhad M (2020) A new machine learning-based healthcare monitoring model for student's condition diagnosis in internet of things environment. Soft Comput 24:17111–17121

23. Alyasseri ZAA, Khader AT, Al-Betar MA, Papa JP, Alomari OA, Makhadmeh SN (2018) Classification of eeg mental tasks using multi-objective flower pollination algorithm for person identification. Int J Integr Eng 10(7)

24. Kumari P, Vaish A (2014) Brainwave based authentication system: research issues and challenges. Int J Comput Eng Appl 4(1):2

25. Adeli H, Ghosh-Dastidar S, Dadmehr N (2007) A wavelet-chaos methodology for analysis of EEGs and EEG subbands to detect seizure and epilepsy. IEEE Trans Biomed Eng 54(2):205–211

26. El-Dahshan E-SA (2011) Genetic algorithm and wavelet hybrid scheme for ECG signal denoising. Telecommun Syst 46(3):209–215

27. Kalaivani M, Kalaivani V, Devi VA (2014) Analysis of EEG signal for the detection of brain abnormalities. Int J Comput Appl Ř Year

28. Al-Qazzaz NK, Hamid Bin Mohd Ali S, Ahmad SA, Islam MS, Escudero J (2015) Selection of mother wavelet functions for multi-channel EEG signal analysis during a working memory task. Sensors 15(11):29015–29035

29. Alyasseri ZAA, Khader AT, Al-Betar MA, Abualigah LM (2017) Ecg signal denoising using β-hill climbing algorithm and wavelet transform. In: ICIT 2017 the 8th international conference on information technology, pp 1–7

30. Rahmani AM, Babaei Z, Souri A (2021) Event-driven iot architecture for data analysis of reliable healthcare application using complex event processing. Cluster Comput 24(2):1347–1360

31. Alyasseri ZAA, Khader AT, Al-Betar MA (2017) Electroencephalogram signals denoising using various mother wavelet functions: a comparative analysis. In: Proceedings of the international conference on imaging, signal processing and communication, pp 100–105

32. Alyasseri ZAA, Khader AT, Al-Betar MA, Awadallah MA (2018) Hybridizing β-hill climbing with wavelet transform for denoising ECG signals. Inf Sci 429:229–246

33. Alyasseri ZAA, Khader AT, Al-Betar MA, Papa JP, Alomari OA, Makhadme SN (2018) An efficient optimization technique of eeg decomposition for user authentication system. In: 2018 2nd International conference on biosignal analysis, processing and systems (ICBAPS), IEEE, pp 1–6

34. Alyasseri ZAA, Khader AT, Al-Betar MA, Abasi AK, Makhadmeh SN (2021) Eeg signal denoising using hybridizing method between wavelet transform with genetic algorithm. In: Proceedings of the 11th national technical seminar on unmanned system technology 2019, Springer, pp 449–469

35. Nguyen P, Kim J-M (2016) Adaptive ECG denoising using genetic algorithm-based thresholding and ensemble empirical mode decomposition. Inf Sci 373:499–511

36. Goldberger AL, Amaral LAN, Glass L, Hausdorff JM, Ivanov PC, Mark RG, Mietus JE, Moody GB, Peng CK, Stanley HE (2000) PhysioBank, physiotoolkit, and physionet: components of a new research resource for complex physiologic signals. Circulation 101(23):e215–e220. circulation Electronic Pages: http://circ.ahajournals.org/content/101/23/e215.full PMID:1085218; https://doi.org/10.1161/01.CIR.101.23.e215

37. Al-Betar MA (2016) b-hill climbing: an exploratory local search. Neural Comput Appl, pp 1–16

38. Alyasseri ZAA, Khader AT, Al-Betar MA, Papa JP, Alomari OA (2018) Eeg feature extraction for person identification using wavelet decomposition and multi-objective flower pollination algorithm, Ieee. Access 6:76007–76024

39. Kumar H, Pai SP, Vijay G, Rao R (2014) Wavelet transform for bearing condition monitoring and fault diagnosis: a review. Int J COMADEM 17(1):9–23

40. Sawant C, Patii HT (2014) Wavelet based ECG signal de-noising. Netw Soft Comput (ICNSC). In: 2014 First international conference on, IEEE, pp 20–24

41. Mamun M, Al-Kadi M, Marufuzzaman M (2013) Effectiveness of wavelet denoising on electroencephalogram signals. J Appl Res Technol 11(1):156–160

42. Al-Kadi MI, Reaz MBI, Ali MAM, Liu CY (2014) Reduction of the dimensionality of the EEG channels during scoliosis correction surgeries using a wavelet decomposition technique. Sensors 14(7):13046–13069

43. Borse S, EEG de-noising using wavelet transform and fast ica. IJISET-Int J Innov Sci Eng Technol

44. Donoho DL, Johnstone JM (1994) Ideal spatial adaptation by wavelet shrinkage. Biometrika 81(3):425–455

45. Singh BN, Tiwari AK (2006) Optimal selection of wavelet basis function applied to ecg signal denoising. Digital Signal Process 16(3):275–287

46. Donoho DL (1995) De-noising by soft-thresholding. IEEE Trans Inf Theory 41(3):613–627

47. Blum C, Roli A (2003) Metaheuristics in combinatorial optimization: overview and conceptual comparison. ACM Comput Surv 35(3):268–308. http://doi.acm.org/10.1145/937503.937505

48. Alyasseri ZAA, Venkat I, Al-Betar MA, Khader AT (2012) Edge preserving image enhancement via harmony search algorithm. in: Data mining and optimization (DMO), 2012 4th conference on, IEEE, pp 47–52

49. Al-Betar MA, Alyasseri ZAA, Khader AT, Bolaji AL, Awadallah MA (2016) Gray image enhancement using harmony search. Int J Comput Intell Syst 9(5):932–944

50. Al-Betar MA, Alyasseri ZAA, Awadallah MA, Doush IA (2020) Coronavirus herd immunity optimizer (chio). Neural Comput Appl, pp 1–32

51. Bolaji AL, Al-Betar MA, Awadallah MA, Khader AT, Abualigah LM (2016) A comprehensive review: Krill herd algorithm (kh) and its applications. Appl Soft Comput 49:437–446

52. Makhadmeh SN, Khader AT, Al-Betar MA, Naim S, Abasi AK, Alyasseri ZAA (2021) A novel hybrid grey wolf optimizer with min-conflict algorithm for power scheduling problem in a smart home. Swarm Evol Comput 60:100793

53. Shehab M, Khader AT, Al-Betar MA (2017) A survey on applications and variants of the cuckoo search algorithm. Appl Soft Comput 61:1041–1059

54. Alomari OA, Makhadmeh SN, Al-Betar MA, Alyasseri ZAA, Doush IA, Abasi AK, Awadallah MA, Zitar RA (2021) Gene selection for microarray data classification based on grey wolf optimizer enhanced with triz-inspired operators. Knowl Based Syst, p 107034

55. Abualigah LM, Khader AT, Al-Betar MA, Alyasseri ZAA, Alomari OA, Hanandeh ES (2017) Feature selection with β-hill climbing search for text clustering application. In: Information and communication technology (PICICT), 2017 Palestinian international conference on, IEEE, pp 22–27

56. Abasi AK, Khader AT, Al-Betar MA, Alyasseri ZAA, Makhadmeh SN, Al-laham M, Naim S (2021) A hybrid salp swarm algorithm with β-hill climbing algorithm for text documents clustering. Algorithms and applications, evolutionary data clustering, p 129

57. Rodrigues D, Silva GF, Papa JP, Marana AN, Yang X-S (2016) EEG-based person identification through binary flower pollination algorithm. Exp Syst Appl 62:81–90

58. Alyasseri ZAA, Khader AT, Al-Betar MA, Abasi AK, Makhadmeh SN (2019) EEG signals denoising using optimal wavelet transform hybridized with efficient metaheuristic methods. IEEE Access 8:10584–10605

59. Jenkal W, Latif R, Toumanari A, Dliou A, El B'charri O, Maoulainine FM (2016) An efficient algorithm of ECG signal denoising using the adaptive dual threshold filter and the discrete wavelet transform. Biocyber Biomed Eng 36(3):499–508

60. Wang J, Ye Y, Pan X, Gao X (2015) Parallel-type fractional zero-phase filtering for ECG signal denoising. Biomed Signal Process Control 18:36–41

61. Schalk G, McFarland DJ, Hinterberger T, Birbaumer N, Wolpaw JR (2004) Bci 2000: a general-purpose brain-computer interface (bci) system. IEEE Trans Biomed Eng 51(6):1034–1043

62. Deb K (2001) Multi-objective optimization using evolutionary algorithms, vol 16. John Wiley & Sons

63. Wilcoxon F (1945) Individual comparisons by ranking methods. Biometrics Bull 1(6):80–83

64. Deb K, Pratap A, Agarwal S, Meyarivan T (2002) A fast and elitist multiobjective genetic algorithm: Nsga-ii. IEEE Trans Evol Comput 6(2):182–197

65. Coello CC, Lechuga MS (2002) Mopso: a proposal for multiple objective particle swarm optimization. In: Proceedings of the 2002 congress on evolutionary computation. CEC'02 (Cat. No. 02TH8600), vol 2, IEEE, pp 1051–1056

66. Bhatnagar A, Gupta K, Pandharkar U, Manthalkar R, Jadhav N (2019) Comparative analysis of ICA, PCA-based EASI and wavelet-based unsupervised denoising for EEG signals. In: Computing, communication and signal processing, Springer, pp 749–759

67. Al-Salman W, Li Y, Wen P (2019) Detecting sleep spindles in EEGs using wavelet fourier analysis and statistical features. Biomed Signal Process Control 48:80–92

68. Luck SJ (2014) An introduction to the event-related potential technique, MIT press

Authors and Affiliations

Zaid Abdi Alkareem Alyasseri[1,2] (ID) · Ahamad Tajudin Khader[3] · Mohammed Azmi Al-Betar[4,5] · Xin-She Yang[6] · Mazin Abed Mohammed[7] · Karrar Hameed Abdulkareem[8] · Seifedine Kadry[9] · Imran Razzak[10]

✉ Zaid Abdi Alkareem Alyasseri
  zaid.alyasseri@uokufa.edu.iq

  Ahamad Tajudin Khader
  tajudin@usm.my

  Mohammed Azmi Al-Betar
  mohbetar@bau.edu.jo

  Xin-She Yang
  x.yang@mdx.ac.uk

  Mazin Abed Mohammed
  mazinalshujeary@uoanbar.edu.iq

  Karrar Hameed Abdulkareem
  Khak9784@mu.edu.iq

  Seifedine Kadry
  seifedine.kadry@noroff.no

  Imran Razzak
  imran.razzak@deakin.edu.au

[1] Center for Artificial Intelligence Technology, Faculty of Information Science and Technology, Universiti Kebangsaan Malaysia, 43600 Bangi, Selangor, Malaysia

[2] ECE Department-Faculty of Engineering, University of Kufa, P.O. Box 21, Najaf, Iraq

[3] School of Computer Sciences, Universiti Sains Malaysia, Pulau Pinang, Malaysia

[4] Artificial Intelligence Research Center (AIRC), College of Engineering and Information Technology, Ajman University, Ajman, UAE

[5] Department of Information Technology, Al-Huson University College, Al-Balqa Applied University, P.O. Box 50 Al-Huson, Irbid, Jordan

[6] School of Science and Technology, Middlesex University, London NW44BT, UK

[7] College of Computer Science and Information Technology, University of Anbar, Anbar 31001, Iraq

[8] College of Agriculture, Al-Muthanna University, Samawah 66001, Iraq

[9] Department of Applied Data Science, Norrof University College, 4608 Kristiansand, Norway

[10] School of Information Technology, Deakin University, Geelong, Australia